

Pyrazine-2-amidoxime Ni(II) Complexes: From Ferromagnetic Cluster to Antiferromagnetic Layer

Guang-Yu An, Cong-Min Ji, Ai-Li Cui, and Hui-Zhong Kou*

Department of Chemistry, Tsinghua University, Beijing 100084, People's Republic of China

Received September 9, 2010

Tetranuclear $[\text{Ni}_4(\text{Hpzaox})_2(\text{pzaox})_2(\text{py})_4](\text{ClO}_4)_2 \cdot 2\text{py}$ (**1**), $[\text{Ni}_4(\text{Hpzaox})_2(\text{pzaox})_2(\text{py})_4](\text{NO}_3)_2 \cdot 4\text{py}$ (**2**), and two-dimensional (2D) $[\text{Ni}_4(\text{Hpzaox})_2(\text{pzaox})_2(\text{H}_2\text{O})_2](\text{NO}_3)_2 \cdot 2\text{H}_2\text{O}$ (**3**) are prepared via the reaction of $\text{NiX}_2 \cdot 6\text{H}_2\text{O}$ and pyrazine-2-amidoxime (H_2pzaox). All compounds contain $[\text{Ni}_4(\text{Hpzaox})_2(\text{pzaox})_2]^{2+}$ fragments, which assemble to form a tetranuclear or polymeric network. Magnetic studies show that the tetranuclear compounds display usual ferromagnetic coupling via the oxime N–O bridges, and the 2D compound displays unusual antiferromagnetic behavior.

Introduction

Oximate-bridged compounds have attracted great attention, because of their interesting magnetic properties.^{1–3} Exciting single-molecule magnets and single-chain magnets have been observed in some oximate-bridged Mn(III) compounds.^{4–6} Current research focuses on the design of molecular assemblies and polymeric networks by adjusting the magnetic precursors and, ultimately, the magnetic properties. In this context, pyrazine-2-amidoxime (H_2pzaox) is a good ligand for the construction of polymeric networks.

Recently, we have found that H_2pyaox can react with Ni(II) in a basic solution, affording single-decker $[\text{Ni}_4(\text{Hpyaox})_2(\text{pyaox})_2]^{2+}$ fragments.^{7,8} Such tetranuclear fragments can further assemble to give a family of single-, double-, and triple-decker Ni(II) complexes.^{7–9} Density functional theory (DFT) calculations and experimental results clearly

show that ferromagnetic coupling between Ni(II) ions through the oximate bridges is relevant to the elongation of N–O bonds, and the switching from antiferromagnetic to ferromagnetic exchange occurs at the N–O bond distance of 1.394 Å.⁸ Herein, we report a novel coordination-driven assembly of three Ni(II) compounds based on H_2pzaox that are similar to H_2pyaox . The pyrazine groups should offer extra donors for the formation of a polymeric network (see Scheme 1).

Results and Discussion

Synthesis. Mixing equimolar $\text{Ni}(\text{NO}_3)_2 \cdot 6\text{H}_2\text{O}$ and H_2pzaox in $\text{MeOH} - \text{H}_2\text{O}$ gave a red brown solution when the pH value of the solution was adjusted to 9–10 using triethylamine, from which a brown microcrystalline solid of the two-dimensional compound $[\text{Ni}_4(\text{Hpzaox})_2(\text{pzaox})_2(\text{H}_2\text{O})_2](\text{NO}_3)_2 \cdot 2\text{H}_2\text{O}$ (**3**) precipitated. Single crystals of compound **3** suitable for structural analysis were grown by the slow evaporation of a $\text{MeCN} - \text{H}_2\text{O}$ solution containing $\text{Ni}(\text{NO}_3)_2 \cdot 6\text{H}_2\text{O}$, H_2pzaox , and imidazole. Imidazole serves as the base for the deprotonation of H_2pzaox during the crystal growth. The purity of the precipitate is verified by the elemental analyses (CHN) and the powder XRD measurement (see Figure S1 in the Supporting Information). Red–brown single crystals of complexes $[\text{Ni}_4(\text{Hpzaox})_2(\text{pzaox})_2(\text{py})_4](\text{ClO}_4)_2 \cdot 2\text{py}$ (**1**) and $[\text{Ni}_4(\text{Hpzaox})_2(\text{pzaox})_2(\text{py})_4](\text{NO}_3)_2 \cdot 4\text{py}$ (**2**) were obtained by the slow diffusion of methanol to the pyridine solution of $\text{NiX}_2 \cdot 6\text{H}_2\text{O}$ (0.2 mmol) and H_2pzaox (0.2 mmol) in a test tube. For the nitrate tetranuclear compound (**2**), a small amount of base (triethylamine in MeOH) should be used to accelerate the reaction. The isolation of compounds **1–3** indicates that tetranuclear $[\text{Ni}_4]^{2+}$ moieties formed in the solution. Note that similar tetranuclear compounds have been prepared by the

*To whom correspondence should be addressed. E-mail: kouhz@mail.tsinghua.edu.cn.

(1) (a) Bodwin, J. J.; Cutland, A. D.; Malkani, R. G.; Pecoraro, V. L. *Coord. Chem. Rev.* **2001**, *216–217*, 489. (b) Marmion, C. J.; Griffith, D.; Nolan, K. B. *Eur. J. Inorg. Chem.* **2004**, 3003–3016.

(2) Chaudhuri, P. *Coord. Chem. Rev.* **2003**, *243*, 143–190.

(3) Milios, C. J.; Stamatos, T. C.; Perlepes, S. P. *Polyhedron* **2006**, *25*, 134–194.

(4) Inglis, R.; Jones, L. F.; Milios, C. J.; Datta, S.; Collins, A.; Parsons, S.; Wernsdorfer, W.; Hill, S.; Perlepes, S. P.; Piligkos, S.; Brechin, E. K. *Dalton Trans.* **2009**, 3403–3412.

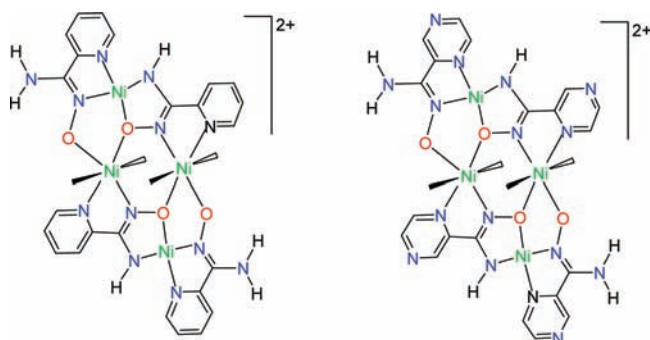
(5) Xu, H.-B.; Wang, B.-W.; Pan, F.; Wang, Z.-M.; Gao, S. *Angew. Chem., Int. Ed.* **2007**, *46*, 7388–7392.

(6) Milios, C. J.; Raptopoulou, C. P.; Terzis, A.; Lloret, F.; Vicente, R.; Perlepes, S. P.; Escuer, A. *Angew. Chem., Int. Ed.* **2004**, *43*, 210–212.

(7) Ji, C.-M.; Yang, H.-J.; Zhao, C.-C.; Tangoulis, V.; Cui, A.-L.; Kou, H.-Z. *Cryst. Growth Des.* **2009**, *9*, 4607–4609.

(8) Kou, H.-Z.; An, G.-Y.; Ji, C.-M.; Wang, B.-W.; Cui, A.-L. *Dalton Trans.* **2010**, 39, 9604–9610.

(9) Papatriantafyllopoulou, C.; Jones, L. F.; Nguyen, T. D.; Matamoros-Salvador, N.; Cunha-Silva, L.; Paz, F. A. A.; Rocha, J.; Evangelisti, M.; Brechin, E. K.; Perlepes, S. P. *Dalton Trans.* **2008**, 3153–3155.

Scheme 1. Drawings of the $[\text{Ni}_4(\text{Hpyaox})_2(\text{pyaox})_2]^{2+}$ Fragment and the $[\text{Ni}_4(\text{Hpzaox})_2(\text{pzaox})_2]^{2+}$ Fragment**Table 1.** Crystallographic Data for Complexes 1–3

	1	2	3
formula	$\text{C}_{50}\text{H}_{48}\text{Cl}_2\text{N}_{22}\text{Ni}_4\text{O}_{22}$	$\text{C}_{60}\text{H}_{58}\text{N}_{26}\text{Ni}_4\text{O}_{10}$	$\text{C}_{20}\text{H}_{26}\text{N}_{18}\text{Ni}_4\text{O}_{14}$
formula weight, fw	1455.85	1538.16	4981.32
temperature, T (K)	293	293	173
crystal system	monoclinic	orthorhombic	monoclinic
space group	$C2/c$	$Cmca$	$P2(1)/c$
a (Å)	15.3903(10)	15.1653(9)	12.249(2)
b (Å)	19.2521(13)	19.4484(8)	9.3940(19)
c (Å)	23.2170(14)	22.8356(9)	15.429(3)
α (deg)	90	90	90
β (deg)	95.504(2)	90	109.29(3)
γ (deg)	90	90	90
V (Å ³)	6847.4(8)	6735.2(6)	1675.7(6)
Z	4	4	2
ρ_{calcd} (g cm ⁻³)	1.412	1.517	1.937
μ (mm ⁻¹)	1.230	1.178	2.308
observed data [$I > 2\sigma(I)$]	4239	2467	2957
goodness of fit, GOF	1.011	0.939	1.087
$R1$ [$I > 2\sigma(I)$]	0.0594	0.0565	0.1179
$wR2$ (all data)	0.1963	0.1599	0.2520

reaction of pyridine-2-amidoxime^{7,8} or 2-pyrimidineamidoxime¹⁰ with Ni^{2+} or Cu^{2+} .

Structural Descriptions. Crystal data and structure refinement details for compounds 1–3 are listed in Table 1. Important structural parameters of complexes 1–3 are collected in Table 2. X-ray crystallography reveals that complexes 1, 2, and 3 show a tetranuclear structure (complexes 1 and 2) and a two-dimensional (2D) polymeric structure (complex 3), where tetranuclear $[\text{Ni}_4(\text{Hpzaox})_2(\text{pzaox})_2]^{2+}$ fragments are present (see Figures 1 and 2). Similar to the H_2pyaox -based $\text{Ni}(\text{II})$ compounds, the $[\text{Ni}_4]^{2+}$ fragments are composed of two square planar $\text{Ni}(\text{II})$ ions and two octahedral $\text{Ni}(\text{II})$ ions, which are connected by two Hpzaox^- and two pzaox^{2-} ligands (see Scheme 1). The coordination sphere of the octahedral $\text{Ni}(\text{II})$ ions is completed by two pyrazine nitrogen atoms for analogous compounds 1 and 2 (Figure 1), and one water oxygen and one pyrazine nitrogen atom from one adjacent $[\text{Ni}_4]^{2+}$ fragment for compound 3 (Figure 2). The use of pyridine in the synthesis precludes formation of the 2D structure, and a tetranuclear compound of pyridine-2-amidoxime have been similarly isolated $[\text{Ni}_4(\text{Hpyaox})_2(\text{pyaox})_2(\text{py})_4](\text{ClO}_4)_2$.⁸

In compound 1, hydrogen bonding between the non-coordinating pyrazine nitrogen atom (N(6)) and the

amino groups of adjacent $[\text{Ni}_4]^{2+}$ group can be observed, connecting the tetranuclear molecules to form a coplanar supramolecular 2D layer (see Figures S2 and S3 in the Supporting Information). The ClO_4^- anions are immersed in the cavities of the layer. Similarly, hydrogen bonds between the noncoordinating pyrazine nitrogen atoms and the amino groups link the molecules, affording a 2D layered network for compound 2 (see Figure S4 in the Supporting Information). In both compounds, the pyrazine groups of Hpyaox^- are not involved in hydrogen bonding interaction.

In compound 3, each tetranuclear $[\text{Ni}_4(\text{Hpzaox})_2(\text{pzaox})_2]^{2+}$ fragment that is surrounded by four $[\text{Ni}_4]^{2+}$ groups uses two pyrazine nitrogen atoms as donors to coordinate with two $\text{Ni}(\text{II})$ ions of two adjacent $[\text{Ni}_4]^{2+}$ fragments, and, in turn, two $\text{Ni}(\text{II})$ ions as acceptors for the coordination of two pyrazine nitrogen atoms from another two adjacent $[\text{Ni}_4]^{2+}$ fragments (see Figure 2 and Figure S5 in the Supporting Information). Consequently, a 2D brick-wall-like layer is obtained. The layer is almost planar, with the nitrate anions situated in the vicinity of the layer (see Figure S6 in the Supporting Information). Interestingly, only the pyrazine groups of pyaox^{2-} bridge $\text{Ni}(\text{II})$ ions.

The oxime N–O bonds of doubly deprotonated pyaox^{2-} ligands are 1.409(4) Å in length, and the $\text{Ni}_{\text{oct}}-\text{N}-\text{O}-\text{Ni}_{\text{oct}}$ torsion angles are 5.15° for compound 1. For compound 2, the N–O bonds that bridge the octahedral $\text{Ni}(\text{II})$ ions have bond distances of 1.402(4) Å, and the corresponding $\text{Ni}_2(\text{NO})_2$ core shows perfect coplanarity (see Figure S7 in the Supporting Information). The N–O bonds of doubly deprotonated pyaox^{2-} ligands are 1.383(12) Å in length, and the $\text{Ni}_{\text{oct}}-\text{N}-\text{O}-\text{Ni}_{\text{oct}}$ torsion angles are 2.23° for compound 3. The adjacent octahedral $\text{Ni}\cdots\text{Ni}$ separations are 3.950(6) Å through the diatomic N–O bridges and 6.960(6) Å through the pyrazine bridges for 3.

Magnetic Properties. Magnetic susceptibility measurements of complexes 1 and 2 show similar magnetic properties (see Figure 3): the $\chi_{\text{m}}T$ value increases steadily as the temperature decreases, which is typical of the presence of overall ferromagnetic coupling. The room-temperature $\chi_{\text{m}}T$ value (2.12 emu K mol⁻¹ for 1 and 2.42 emu K mol⁻¹ for 2) is in good agreement with the calculated spin-only value (2.0 emu K mol⁻¹) for two uncoupled octahedral $\text{Ni}(\text{II})$ ions with $g = 2.0$. The rapid decrease of $\chi_{\text{m}}T$ at low temperature should be due to the zero-field splitting (ZFS) effect of $\text{Ni}(\text{II})$, the Zeeman effect, and/or intercluster antiferromagnetic interaction. The fit of the $\chi_{\text{m}}^{-1}-T$ curve to the Curie–Weiss law gave Weiss constants of +0.26 K and +4.7 K for compounds 1 and 2, respectively, suggesting the existence of overall ferromagnetic coupling in these compounds.

The magnetic susceptibilities (2–300 K) of complexes 1 and 2 can be fitted by the expressions derived from the isotropic exchange spin Hamiltonian¹¹ for dimeric $\text{Ni}(\text{II})$ complexes $\hat{H} = -2J\hat{S}_{\text{Ni}_1}\hat{S}_{\text{Ni}_2} - D_{\text{Ni}_1}(\hat{S}_{\text{Ni}_1}^2 + \hat{S}_{\text{Ni}_2}^2) - g\beta H(\hat{S}_{\text{Ni}_1} + \hat{S}_{\text{Ni}_2}) - zJ'\hat{S}_z\langle\hat{S}_z\rangle$, involved the intermolecular exchange interaction (zJ') in the molecular-field approximation, giving the parameters of $J = 1.19(5) \text{ cm}^{-1}$, $g = 2.05(1)$, $D_{\text{Ni}} = 9.8(5) \text{ cm}^{-1}$, $zJ' = -0.21(1) \text{ cm}^{-1}$ for 1

(10) Gole, B.; Chakrabarty, R.; Mukherjee, S.; Song, Y.; Mukherjee, P. S. *Dalton Trans.* **2010**, 39, 9766–9778.

(11) Wang, Q.-L.; Yu, L.-H.; Liao, D.-Z.; Yan, S.-P.; Jiang, Z.-H.; Cheng, P. *Helv. Chim. Acta* **2003**, 86, 2441–2451.

Table 2. Comparison of Bond Distances and Bond Angles for Complexes 1–3

	1	2	3
Bond Distances (Å)			
Ni _{sq} –N/O	1.824(3)–1.888(4)	1.819(3)–1.879(3)	1.841(8)–1.884(11)
Ni _{oct} –N/O	2.012(3)–2.174(5)	2.000(3)–2.166(4)	2.018(8)–2.136(11)
N–O ^a	1.409(4)	1.402(4)	1.383(12)
Ni _{oct} ···Ni _{oct} ^b	4.004(1)	4.010(1)	3.950(6)
Bond Angle (deg)			
Ni _{oct} –N–O–Ni _{oct}	5.15	0	2.23

^a N–O groups bridging the octahedral Ni(II) ions. ^b The intramolecular Ni···Ni separations through the N–O bridges.

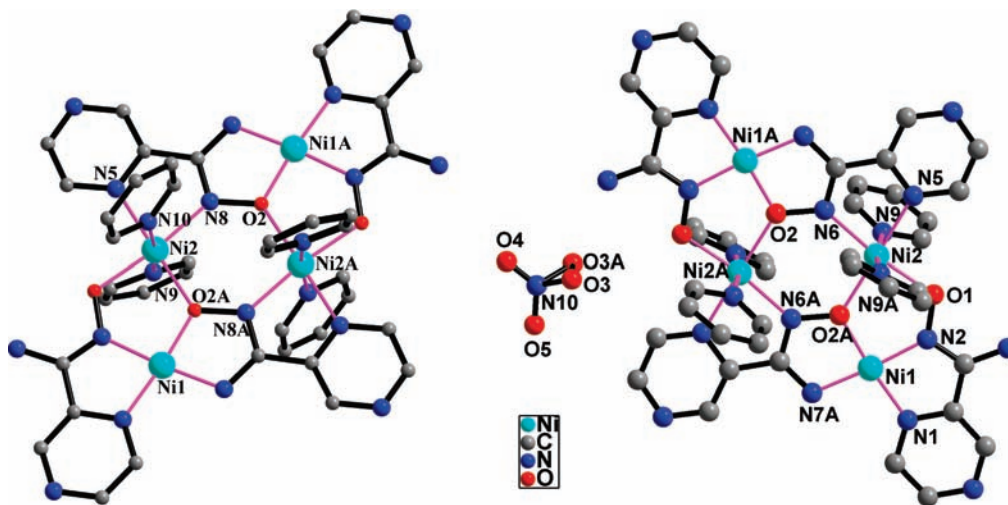


Figure 1. Crystal structure of the tetranuclear compounds **1** (left) and **2** (right). One oxygen atom of the nitrate anions is disordered over two positions in compound **2**.

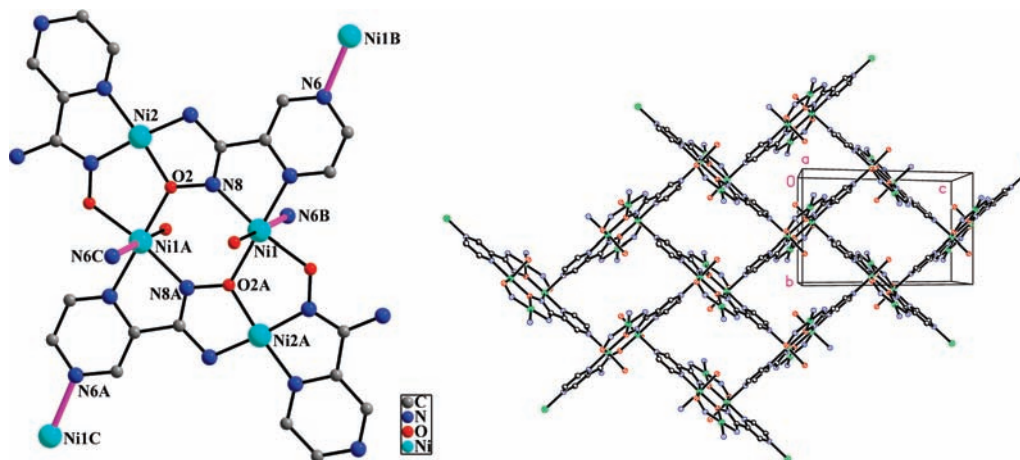


Figure 2. Left: coordination environment of Ni(II) ions in complex **3** (for the sake of clarity, hydrogen atoms are not shown). Selected bond distances and torsion angles: N(8)–O(2), 1.383(12) Å, Ni(1)–N(8)–O(2)–Ni(1A), 2.23°. Right: 2D layered structure of complex **3** (for the sake of clarity, some atoms of the ligands Hpzaox[−] and pzaox^{2−} are not shown).

and $J = 4.8(2) \text{ cm}^{-1}$, $g = 2.15(1)$, $D_{\text{Ni}} = 1.4(2) \text{ cm}^{-1}$, $zJ' = -0.25(2) \text{ cm}^{-1}$ for **2**. The J values are comparable with that of the analogous pyridine-2-amidoxime Ni₄ compounds ($1.6\text{--}6.3 \text{ cm}^{-1}$).^{7,8}

However, the magnetic behavior of the 2D compound **3** is different. The decrease in $\chi_{\text{m}}T$ with decreasing temperature implies the existence of global antiferromagnetic

interaction in compound **3**. The fit of the $\chi_{\text{m}}^{-1}\text{--}T$ curve to the Curie–Weiss law gives a Weiss constant of -2.6 K , suggesting the existence of overall antiferromagnetic coupling. In compound **3**, two magnetic coupling pathways concur (i.e., magnetic coupling through the oximate and through the pyrazine bridges). Therefore, two approximate fitting methods have been tried. First, neglecting

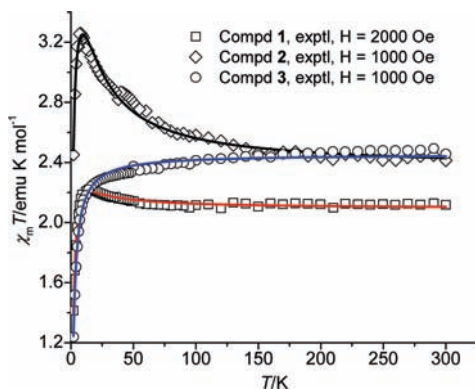


Figure 3. Temperature dependence of $\chi_m T$ for complexes **1–3**. The solid lines represent the best-fit results with the parameters described in the text.

the ZFS effect and treating the magnetic coupling through pyrazine pathway as a minor factor, the dimer model based on the isotropic exchange spin Hamiltonian $\hat{H} = -2J\hat{S}_{\text{Ni}} \cdot \hat{S}_{\text{Ni}'} - g\beta H(\hat{S}_{\text{Ni}} + \hat{S}_{\text{Ni}'}) - zJ'\hat{S}_z(\hat{S}_z)$ was first tried yielding the least-squares fitting parameters of $J = -0.35(5) \text{ cm}^{-1}$, $zJ' = -0.23(4) \text{ cm}^{-1}$, $g = 2.21(1)$. J represents the intracuster Ni(II)–Ni(II) magnetic coupling via the oximate bridges, and zJ' the intercluster magnetic coupling via pyrazine and hydrogen-bonding pathways. Comparable fitting results were obtained by considering ZFS as the major effect and the magnetic interactions as the minor effect with $D_{\text{Ni}} = 2.3(4) \text{ cm}^{-1}$, $zJ' = -0.20(1) \text{ cm}^{-1}$, $g = 2.21(1)$.¹² Both fitting results clearly show that the magnetic exchange pathways should transmit weak antiferromagnetic interaction (small $|J|$ and $|zJ'|$), and that the magnetic coupling via the oximate bridges is antiferromagnetic in compound **3**.

The field-dependent magnetizations measured at 2 K for compounds **1–3** show regular increases in magnetization with increasing applied external magnetic field (see Figure 4). The magnetization values for compounds **1**, **2**, and **3** amount to $3.1 N\beta$, $4.28 N\beta$, and $3.2 N\beta$ at 70 kOe, respectively. The curve of compound **2** lies above the Brillouin function for two uncoupled $S = 1 \text{ Ni}^{2+}$ ions, indicating the presence of ferromagnetic coupling in the compound. Magnetization data for complexes **1** and **3** are lower than that calculated, indicating the presence of intermolecular antiferromagnetic coupling and/or a significant ZFS effect in compound **1**. At low magnetic fields, the experimental data of compound **3** are less than that of compounds **1** and **2**, suggesting the antiferromagnetic property of compound **3**.

Pyrazine-bridged Ni(II) compounds have shown weak antiferromagnetic coupling, with an exchange constant of $< 1.32 \text{ cm}^{-1}$.¹³ However, a stronger antiferromagnetic exchange (3.8 cm^{-1}) has been observed in TPPZ

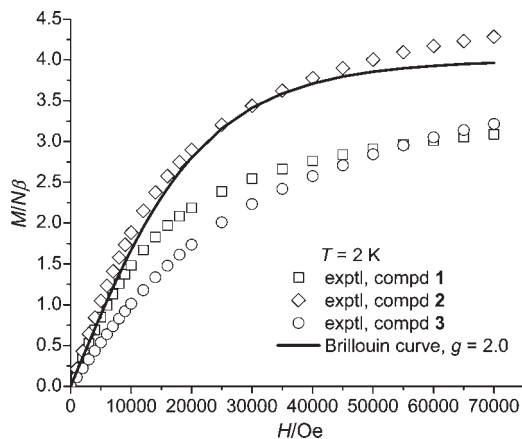


Figure 4. Field-dependence of magnetization at 2 K for complexes **1–3**. The solid line denotes the Brillouin function for two uncoupled $S = 1 \text{ Ni}^{2+}$ ions.

Ni(II) compounds (where TPPZ = 2,3,5,6-tetra(2-pyridyl)pyrazine).¹⁴ This may be due to the good coplanarity between pyrazine ring and the NiN_4 chromophore. Significantly, the pyrazine ring in TPPZ is not planar, which may further affect the magnitude of the magnetic coupling.

Previous DFT calculations on an oximate-bridged dinuclear Ni(II) compound show that, with the decrease in the bond lengths of N–O, the spin population on Ni^{2+} ions does not change significantly, but the spin population on the N and O atoms increases.⁸ The increase in spin delocalization of Ni^{2+} toward N–O bridges would enhance the antiferromagnetic coupling between Ni^{2+} ions and induce the change in total magnetic interaction from ferromagnetic character to antiferromagnetic character. The magnetic properties of compounds **1** and **2** are consistent with the critical value of 1.394 \AA for the bond distances of the bridging N–O groups. Complex **3** has N–O bond distances of $1.383(12) \text{ \AA}$, which fall in the range of antiferromagnetic property.

Conclusion

Initially, using pyrazine-2-amidoxime, we have isolated two tetranuclear Ni(II) clusters and a novel two-dimensional (2D) molecular brick wall, which respectively display overall ferromagnetic and antiferromagnetic properties. Magnetostructural studies further verify that the bond distances of bridging oxime groups have a significant effect on the magnetism of Ni(II) compounds. However, the presence of the pyrazine bridging pathways in the 2D compound complicates the magnetism; therefore, examples that contain solely oximate-bridged Ni(II) compounds are anticipated to completely solve the problem.

Experimental Section

Materials and Synthesis. All the starting chemicals were analytical reagent (AR) grade and used as-received. H_2pzaox was prepared as colorless needle crystals, according to the literature method for the synthesis of H_2pyaiox .¹⁵ Hydroxylamine

(12) Kahn, O. *Molecular Magnetism*; VCH Publishers: New York, 1993.

(13) (a) James, M. *Aust. J. Chem.* **2002**, *55*, 219. (b) Otieno, T.; Thompson, R. C. *Can. J. Chem.* **1995**, *73*, 275. (c) Lloret, F.; Julve, M.; Cano, J.; De Munno, G. *Mol. Cryst. Liq. Cryst.* **1999**, *334*, 569. (d) Cati, D. S.; Ribas, J.; Ribas-Arino, J.; Stoeckli-Evans, H. *Inorg. Chem.* **2004**, *43*, 1021–1030. (e) Wriedt, M.; Jess, I.; Näther, C. *Eur. J. Inorg. Chem.* **2009**, 1406–1413. (f) Wang, Q.-L.; Qi, F.; Yang, G.; Liao, D.-Z.; Yang, G.-M.; Ren, H.-X. *Z. Anorg. Allg. Chem.* **2010**, *636*, 634–640. (g) Klingele, J.; Boas, J. F.; Pilbrow, J. R.; Moubaraki, B.; Murray, K. S.; Berry, K. J.; Hunter, K. A.; Jameson, G. B.; Boyd, P. D. W.; Brooker, S. *Dalton Trans.* **2007**, 633–645.

(14) (a) Neels, A.; Neels, B. M.; Stoeckli-Evans, H.; Clearfield, A.; Poojary, D. M. *Inorg. Chem.* **1997**, *36*, 3402–3409. (b) Graf, M.; Stoeckli-Evans, H.; Escuer, A.; Vicente, R. *Inorg. Chim. Acta* **1997**, *257*, 89–97. (c) Callejo, L. M.; Madariaga, G.; Lezama, L.; Fidalgo, L.; Pinta, N.; De la, Cortes, R. *Inorg. Chem.* **2010**, *49*, 5353–5355.

hydrochloride (0.69 g, 10 mmol) and an excess of triethylamine (1.1 g, 11 mmol) were added to a solution of cyanopyrazine (1.05 g, 10 mmol) in methanol (30 mL), and the mixture was stirred at room temperature for 2 h. A white needle-shaped crystalline product was deposited from the solution, which was collected by suction filtration and washed with cold methanol. Pure product can be obtained by recrystallization of the crude product in water. Yield, 85%; melting point (mp), 188 °C. Main infrared (IR) bands (cm^{-1}): $\nu(\text{C}=\text{N})$, 1671(vs), 1660(vs); $\nu(\text{N}-\text{O})$, 1484(vs).

Caution! Perchlorate salts of metal complexes with organic ligands are potentially explosive. They should be handled in small quantities with care.

[Ni₄(Hpzaox)₂(pzaox)₂(py)₄](ClO₄)₂·2py (1). Red–brown single crystals of complex **1** were obtained via the slow diffusion of methanol (3 mL) to the pyridine solution (5 mL) of Ni(ClO₄)₂·6H₂O (0.2 mmol) and H₂pzaox (0.2 mmol) in a test tube. Yield, ca. 40%. Main IR bands (cm^{-1}): $\nu(\text{C}=\text{N})$, 1634(vs), 1600(vs); $\nu(\text{N}-\text{O}, \text{oximato})$, 1480(vs); $\nu(\text{Cl}-\text{O})$, 1100(br).

[Ni₄(Hpzaox)₂(pzaox)₂(py)₄](NO₃)₂·4py (2). Red–brown single crystals of complex **1** were obtained by the slow diffusion of triethylamine (0.1 mL) in methanol (3 mL) to the pyridine solution (5 mL) of Ni(NO₃)₂·6H₂O (0.2 mmol) and H₂pzaox (0.2 mmol) in a test tube. Yield, ca. 40%. Main IR bands (cm^{-1}): $\nu(\text{C}=\text{N})$, 1627(vs), 1600(vs); $\nu(\text{N}-\text{O}, \text{oximato})$, 1480(vs); $\nu(\text{N}-\text{O}, \text{NO}_3^-)$, 1380(br).

[Ni₄(Hpzaox)₂(pzaox)₂(H₂O)₂](NO₃)₂·2H₂O (3). Mixing equimolar Ni(NO₃)₂·6H₂O and H₂pzaox in MeCN–H₂O gave a red–brown solution when the pH value of the solution was adjusted to 9–10, using triethylamine, from which a brown microcrystalline solid of compound **3** precipitated. Small single crystals of compound **3** suitable for structural analysis were grown by the slow evaporation of a MeCN–H₂O solution containing Ni(NO₃)₂·6H₂O, H₂pzaox and imidazole. Yield, 60%. Anal. Calcd for C₂₀H₂₈N₁₈Ni₄O₁₅ (3·H₂O): C, 24.20; H, 2.84; N, 25.41. Found: C, 24.5; H,

2.5; N, 24.9. $\nu(\text{C}=\text{N})$, 1630(vs), 1610(sh); $\nu(\text{N}-\text{O}, \text{oximato})$, 1478(vs); $\nu(\text{N}-\text{O}, \text{NO}_3^-)$, 1384(br).

Physical Measurements. Elemental analyses (C,H,N) of compound **3** were performed with an Elementar Vario EL analyzer. IR spectra were performed on a Nicolet Model Magna-IR 750 spectrometer in the 4000–650 cm^{-1} region. The room-temperature powder X-ray diffraction (XRD) analysis for compound **3** was performed over the angular range $5^\circ < 2\theta < 40^\circ$ with a 0.02° step on a Bruker D8-Discover high-resolution diffractometer with Cu K α source ($\lambda = 1.5406 \text{ \AA}$). Temperature- and field-dependent magnetic susceptibility measurements were performed on a Quantum Design MPMS SQUID magnetometer from 2 K to 300 K. Some crystals of compounds **1** and **2** and microcrystals of compound **3** were used for magnetic measurements. The experimental susceptibilities were corrected for the diamagnetism of the constituent atoms (from Pascal's Tables).

Single-crystal X-ray data were collected on a Rigaku Model R-Axis Rapid IP diffractometer (**1** and **2**) at room temperature and on a Rigaku Model Saturn724+ system for compound **3** at 173 K. The structures were solved by direct method SHELXS-97 and refined by full-matrix least-squares (SHELXL-97) on F^2 . Hydrogen atoms were added geometrically and refined using a riding model. One oxygen atom of the nitrate anion in complex **2** experiences disorder over two symmetry-related positions. The crystals of compound **3** diffract weakly, because of the small size of the crystals; therefore, the crystal data are not high-quality.

Acknowledgment. The authors would like to acknowledge the financial support of the National Natural Science Foundation of China (Project Nos. 50873053 and 20921001).

Supporting Information Available: Powder XRD pattern of the powdered sample for compound **3**. Molecular structures of compounds **1–3**. An X-ray crystallographic file (CIF) also is provided. This material is available free of charge via the Internet at <http://pubs.acs.org>.

(15) Fish, P. V.; Allan, G. A.; Bailey, S.; Blagg, J.; Butt, R.; Collis, M. G.; Greiling, D.; James, K.; Kendall, J.; McElroy, A.; McCleverty, D.; Reed, C.; Webster, R.; Whitlock, G. A. *J. Med. Chem.* **2007**, *50*, 3442–3456.